

70331

This is a preprint of a paper intended for publication in a journal or proceedings. Since changes may be made before publication, this preprint is made available with the understanding that it will not be cited or reproduced without the permission of the author.

UCRL - 76033  
**PREPRINT**

Conf-741109--1



**LAWRENCE LIVERMORE LABORATORY**  
*University of California / Livermore, California*

**MASTER**

Measurements of Neutron Emission Spectra  
from 14-MeV Neutrons on Thick Targets

J. D. Anderson  
L. F. Hansen  
and  
C. Wong

October 1974

**NOTICE**

This report was prepared as an account of work sponsored by the United States Government. Neither the United States nor the United States Atomic Energy Commission, nor any of their employees, nor any of their contractors, subcontractors, or their employees, makes any warranty, express or implied, or assumes any legal liability or responsibility for the accuracy, completeness or usefulness of any information, apparatus, product or process disclosed, or represents that its use would not infringe privately owned rights.

This paper was prepared to be presented at the  
International Symposium on Radiation Physics (1974)  
November 30 - December 4

394

Subject Category  
2. Neutron Transport in Bulk Media

International Symposium on Radiation Physics (1974)

November 30 to December 4

Bose Institute, Calcutta - 700009, India

Measurements of Neutron Emission Spectra  
from 14-MeV Neutrons on Thick Targets\*

J. D. Anderson, L. F. Hansen and C. Wong

Lawrence Livermore Laboratory, Livermore California 94550

#### Abstract

Spherical assemblies of materials ranging from 1 to 5 mean-free-paths have been bombarded with a centered 14-MeV neutron source. The emitted neutron energy spectra were measured using time-of-flight techniques (2-10 ns FWHM system resolution) in a geometry where the flight path (7-10 meters) is long compared to the dimensions of the spherical targets. It has proved possible to measure emission spectra from 14 MeV (the source energy) down to 10 keV. Two detector systems were used: a NE 213 liquid scintillator for high-energy neutron measurements ( $E_n > 1$  MeV) and a  ${}^6\text{Li}$  glass detector for the low-energy measurements ( $10 \text{ keV} < E_n < 1 \text{ MeV}$ ).

Measured spectra will be presented for materials of particular interest to controlled thermonuclear reactors, e.g.,  ${}^6\text{Li}$ ,  ${}^7\text{Li}$ , C and Fe. The examples cited are chosen to emphasize the usefulness of these bulk measurements in 1) checking transport codes 2) evaluating neutron cross sections and 3) assessing the reliability of computational and/or reaction models.

\*Work performed under the auspices of the U.S. Atomic Energy Commission.

## Introduction

Since the initiation of the pulsed sphere program at the Lawrence Livermore Laboratory in 1967, extensive measurements have been made of the neutron spectra from spherical targets bombarded with a centered 14-MeV neutron source. Neutron emission spectra have been measured for material ranging from hydrogen to lead for thicknesses between 1 and 5 mfp. The objective of the program has been to measure the neutron spectra with adequate resolution in order to make available test cases for the neutron transport codes and input neutron cross sections. The resolution has been sufficiently good to enable us to check not only the total cross sections as function of energy but also the 14-MeV differential elastic and inelastic cross sections to low lying strongly excited levels.<sup>1,2,3</sup> In this paper, the discussion is restricted to materials of interest to controlled thermonuclear reactors such as  ${}^6\text{Li}$ ,  ${}^7\text{Li}$ , C and Fe.

## Experimental Method

The measurements have been carried out using time-of-flight techniques for a flight path between 7 and 10 meters. Nominal 14-MeV neutrons are obtained from the  $\text{T}(d,n){}^4\text{He}$  reaction, the 400-keV deuterons being produced by the Livermore insulated core transformer (ICT) accelerator. The deuteron beam, pulsed and bunched according to the requirements of the measurements, struck a tritium-titanium target with a tungsten backing 2.06 cm in diameter and 0.051 cm thick. This target is mounted at the end of a low-mass assembly and is positioned at the center of the spheres. The neutron production is monitored by counting the associated alpha particles with a thin lithium-drifted silicon solid-state detector set at  $174^\circ$  with respect to the deuteron beam line. A schematic drawing of the experimental setup is shown in Fig. 1.

The experimental facility is fully described in Ref. 4.

For spectra measurements between 1 and 15 MeV (high energy region) NE 213 scintillators were positioned at 30 and 120 degrees with respect to the deuteron beam line. Early measurements employed a Pilot B scintillator at 30 degrees, which has since been replaced with NE 213 resulting in much lower time independent  $\gamma$ -ray background because of the use of pulse shape discrimination. For neutrons between 10 keV and 1 MeV (low energy region) a  $^6\text{Li}$  glass detector was employed. A description of the different detector systems and their efficiencies are found in Ref. 4.

#### Experimental Results and Discussion

Over sixty neutron spectra<sup>4</sup> have been measured including  $^6\text{Li}$ ,  $^7\text{Li}$ , Be, C, N, O, Mg, Al, Ti, Fe and Pb and some compounds such as water, heavy water, polyethylene, teflon and concrete. The measurements for water and heavy water investigated the transport of 14-MeV neutrons in hydrogen and deuterium since the transport of 14-MeV neutrons in oxygen has been studied earlier.<sup>2</sup> Furthermore, the study<sup>5</sup> of 14-MeV neutron transport in water is in itself important because of biomedical and shielding applications.

The future development of fusion reactors employing tritium and deuterium brings into focus a large number of problems dealing with the interaction of 14-MeV neutrons with different materials. Questions related to neutron multiplication and tritium breeding in the blanket can be reliably answered only if the codes can correctly calculate the transport of 14-MeV neutrons in  $^6\text{Li}$  and  $^7\text{Li}$ . Questions related to the shielding of the superconductor magnet to minimize radiation damage and heating of the

cryogenic coils and radiation damage to the structural material of the blanket and first wall which separates the plasma from the blanket, can be resolved only if the transport of neutrons in materials used in a thermonuclear reactor can be correctly calculated. Molybdenum<sup>6</sup> and mixtures of stainless steel and boron carbide<sup>7</sup> are examples of some suggested structural materials. All feasibility studies and optimum design studies of the blanket and walls of the reactor found in the literature have been obtained from neutron transport calculations using libraries such as ENDF/B.<sup>8</sup> The accuracy of these calculations can be checked by ascertaining how well the transport code reproduces the 14-MeV integral measurements of the neutron emission spectra from materials used in fusion reactors.

Measurements will now be presented on C, Fe, <sup>6</sup>Li and <sup>7</sup>Li to illustrate what can be learned from a comparison between measurements and calculations. Figure 2 shows the neutron emission spectrum from 1.3 mfp of carbon bombarded with a nominal 14-MeV neutron source (at 120° the energy of the neutrons from the T(d,n)<sup>4</sup>He reaction is 13.7 MeV). In carbon a comparison<sup>1</sup> between measurements and calculations was used to test in detail the following aspects of the calculations:

- 1) The 14-MeV differential elastic cross sections. The 14-MeV elastically scattered neutrons contribute scattered neutrons between 9 and 13 MeV. Experimental points beyond 13 MeV result from the energy spread associated with the time resolution of the measurements.
- 2) The angular distribution of neutrons inelastically scattered from the 4.43-MeV level. These differential cross sections contribute scattered neutrons between 6 and 9 MeV.

3) The total cross section as a function of energy. The window effect due to a minimum in the total cross section can be seen as a peak in the neutron spectrum around 3 MeV; this peak can be reproduced by the calculations only if the number of neutron energy groups are sufficiently large to reproduce this structure in the total cross section.

4) The magnitude of the total cross section at 13.7 MeV. This cross section was tested by seeing how the height of the transmitted peak was reproduced as a function of increasing the number of mean free paths.

If stainless steel were chosen as a structural and shielding material for fusion reactors, the neutronic behavior of this material can be studied by comparing the calculations with experimental results available for iron.<sup>3</sup> Stainless steel is greater than 55% iron and 20 to 40% chromium and nickel. One expects that the neutron emission spectra from these latter metals will not be very different from Fe. The rest of the components such as P, S and Si do not contribute more than 1%. The exception is Mn whose percentage varies between 1 and 10% depending upon the type of stainless steel. Below 100 keV, the stainless steel spectrum may differ significantly from the Fe spectrum because of the large Mn capture cross section.

Figure 3 shows the neutron emission spectra from 2.9 mfp of Fe (13.4 cm sphere radius) for neutron energies between 10 keV and 15 MeV. The gap between 1 and 2 MeV can be removed by lowering the NE 213 detector bias. The cross sections in the ENDF/B-III (Ref. 8) libraries were checked by comparing their predictions with these measurements. A detailed discussion can be found in Ref. 3. The main conclusions were that the ENDF/B-III library reproduces, rather well, the low energy region of the measurements ( $E \leq 1$  MeV), but that the high energy neutrons between 2 and 10 MeV were

underestimated by factors of 2 to 5. This discrepancy also showed up in a comparison between calculations and measurements for the 1, 3 and 5 mfp Fe spheres. To remedy this deficiency the ENDF/B-IV library, recently released,<sup>9</sup> will increase the number of high energy neutrons. Calculations with the new ENDF/B-IV have not yet been carried out for Fe to check with measurements. (Reference 3 also discusses how a combination of the statistical, pre-equilibrium and direct reaction models can account for the observed neutron spectrum.)

Figures 4 and 5 show the neutron energy spectra from 0.5 and 1.6 mfp of  ${}^6\text{Li}$  and  ${}^7\text{Li}$ . The spectra appear similar despite the fact that the level structures for these two nuclei are rather different. This is partially a result of the large kinematic energy spread ( $15 \leq E_n \leq 6$  MeV) of the elastically scattered neutrons between 0 and  $180^\circ$  such that the features of the elastic differential cross sections are superimposed on peaks resulting from inelastic scattering from the 2.184- and 3.560-MeV levels in  ${}^6\text{Li}$  and the 0.478-, 4.63- and 7.47-MeV levels in  ${}^7\text{Li}$ . The ENDF/B-IV is able to reproduce with excellent agreement the 1.6-, 1.1- and 0.5-mfp  ${}^7\text{Li}$  measurements. For  ${}^6\text{Li}$  the ENDF/B-IV calculations underestimate the neutrons emitted between 7 and 11 MeV by as much as a factor of 2.

Figure 6 shows the measured time-of-flight spectra from 1.6 mfp of  ${}^7\text{Li}$  and the corresponding energy spectra. The transformation from time to energy was done relativistically assuming a flight path equal to the distance between the detector and tritium target. This procedure is strictly valid only if the sphere radius is much smaller than the distance between detector and tritium target. Figure 6 also shows the Monte Carlo

neutron transport calculations run with the code TART<sup>10</sup> and the ENDF/B-IV cross sections<sup>9</sup> edited on energy and time-of-arrival. The good agreement in both energy and time-of-flight spectra checks the ENDF/B-IV cross sections and shows that the energy spectrum obtained from the time-of-flight measurements can be used reliably to check the Monte Carlo calculations for a given material. This type of comparison is most useful for those users working with non-time-dependent transport calculations.



## References

1. L. F. Hansen, J. D. Anderson, E. Goldberg, E. F. Plechaty, M. L. Stelts and C. Wong, *Nucl. Sci. and Eng.* 35, 227 (1969).
2. L. F. Hansen, J. D. Anderson, E. Goldberg, J. L. Kammerdiener, E. F. Plechaty and C. Wong, *Nucl. Sci. and Eng.* 40, 262 (1970).
3. L. F. Hansen, J. D. Anderson, P. S. Brown, R. J. Howerton, J. L. Kammerdiener, C. M. Logan, E. F. Plechaty and C. Wong, *Nucl. Sci. and Eng.* 51, 278 (1973).
4. C. Wong, J. D. Anderson, P. S. Brown, L. F. Hansen, J. L. Kammerdiener, C. M. Logan and B. A. Pohl, Livermore Pulsed Sphere Program, Program Summary Through July 1971. UCRL-51144.
5. M. L. Stelts, J. D. Anderson, L. F. Hansen, E. F. Plechaty and C. Wong, *Nucl. Sci. and Eng.* 46, 53 (1971).
6. D. Steiner, *Nuclear Applications and Technology*, Vol. 9, 83 1970.
7. M. A. Abdou and C. W. Maynard, Important Considerations in the Design of a Shield for a CTR Magnet ANS Transactions, Vol. 17, No. 1, p 32, 1974.
8. ENDF/B Library, Summary Documentation Assembly by D. Ozev and D. Garber, 1973.
9. R. W. Roussin and J. B. Wright, Defense Nuclear Agency Working Cross Section Library, ORNL-RSIC-34, Vol. 1, June 1974.
10. E. F. Plechaty and J. R. Kimlinger, "TART Monte Carlo Neutron-Transport Code," UCIR-522, Lawrence Livermore Laboratory (1971).

## Figure Captions

Fig. 1. Schematic drawing of the experimental setup..

Fig. 2. Measured high energy neutron spectra at  $120^\circ$  from 1.3 mfp of carbon plotted as a function of emitted neutron energy.

Fig. 3. Composite neutron spectra from 2.9 mfp of iron plotted as a function of emitted neutron energy.

Fig. 4. Measured high energy neutron spectra from 0.5 mfp of  $^6\text{Li}$  at  $120^\circ$  and 1.6 mfp of  $\text{Li}$  at  $30^\circ$  plotted as a function of emitted neutron energy.

Fig. 5. Measured high energy neutron spectra from 0.5 mfp of  $^7\text{Li}$  at  $120^\circ$  and 1.6 mfp of  $^7\text{Li}$  at  $30^\circ$  plotted as a function of emitted neutron energy.

Fig. 6. Comparison between the measurements of the high energy neutron spectra at  $30^\circ$  from 1.6 mfp of  $^7\text{Li}$  plotted as a function of neutron arrival time (above) and as a function of neutron energy (below) and the respective TART calculations using the ENDF/B-IV Library. In the energy plot the calculations and measurements do not agree above 14 MeV due to the finite time resolution of the experiment. However, the integrals are in good agreement.

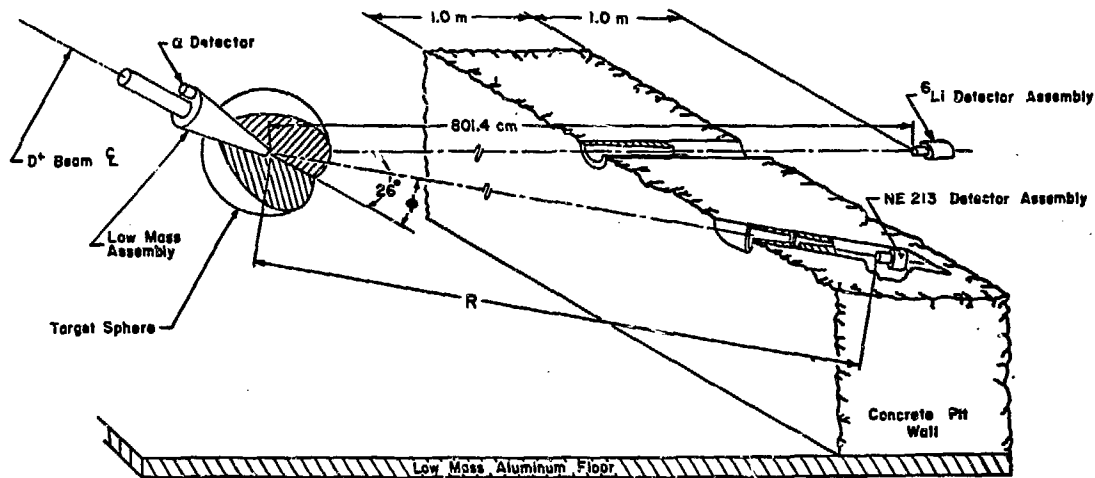


Fig. 1

$\phi$	R
30°	766.0 cm
120°	975.2 cm

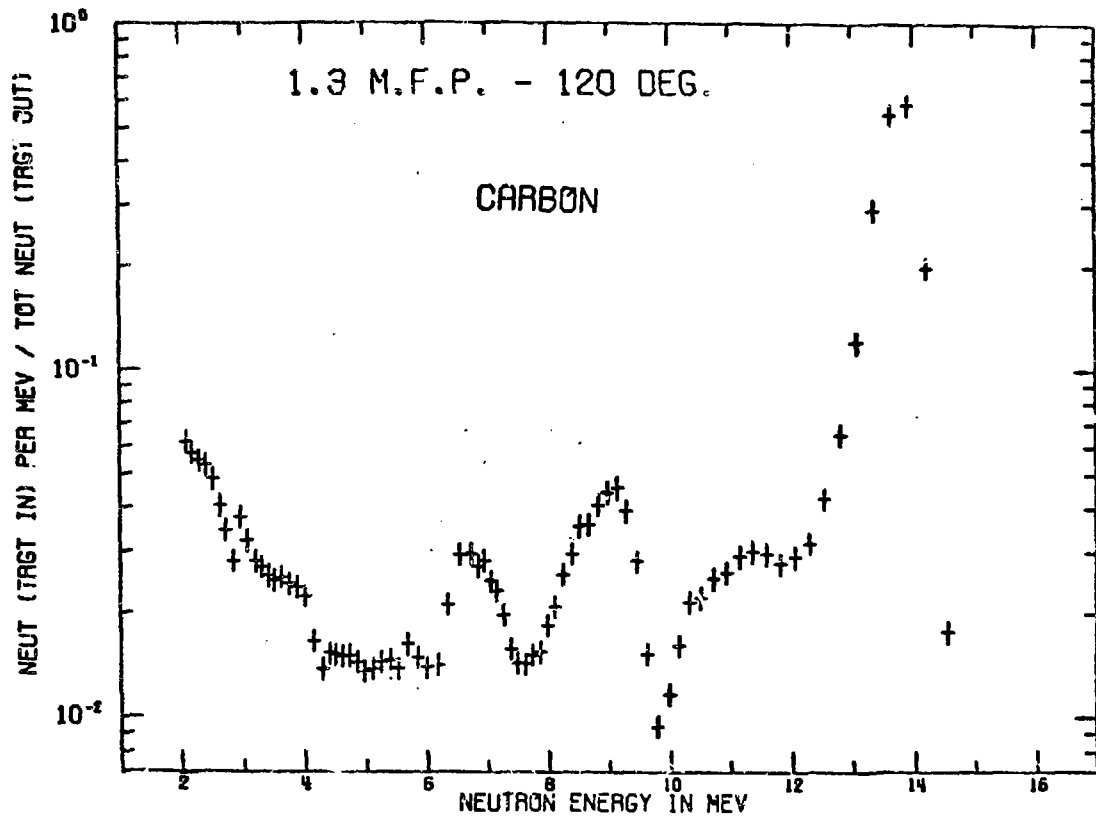


Fig. 2

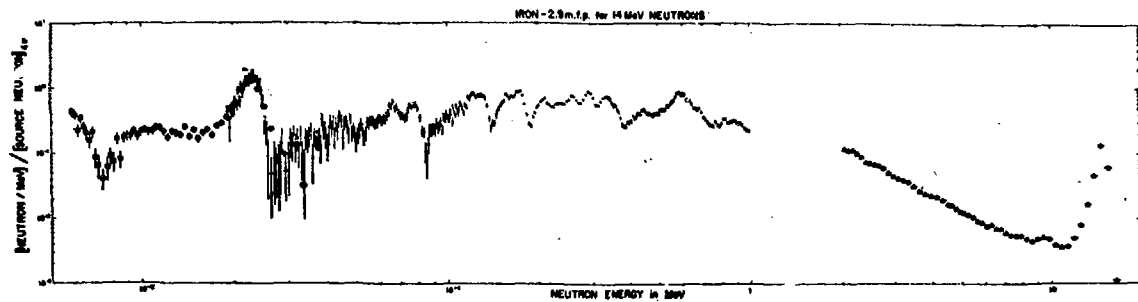


Fig. 3

# LITHIUM 6

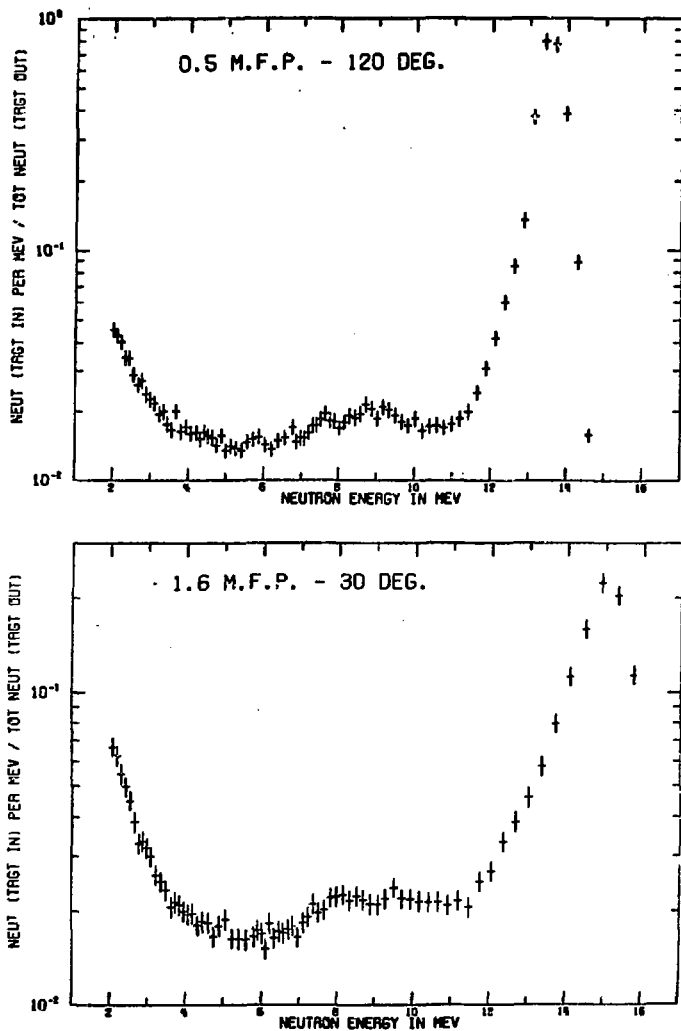


Fig. 4

# LITHIUM 7

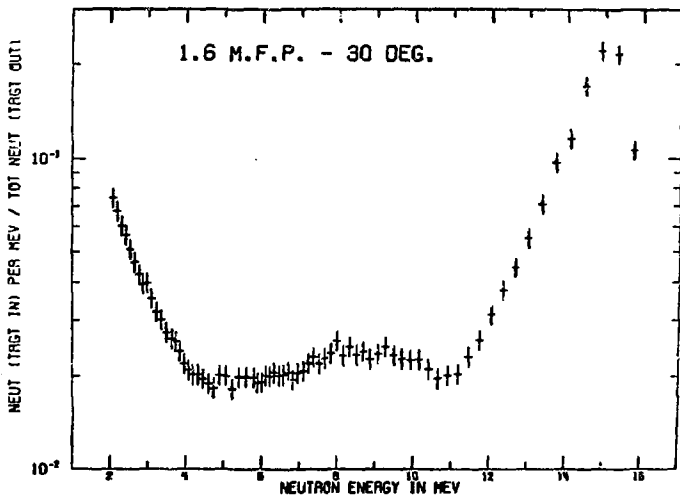
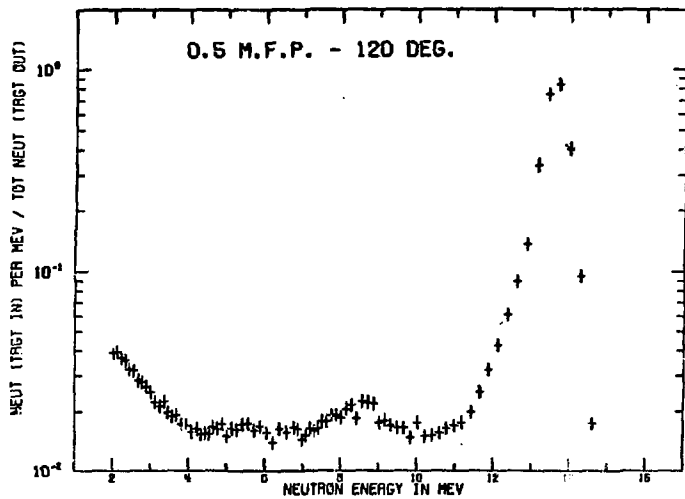


Fig. 5

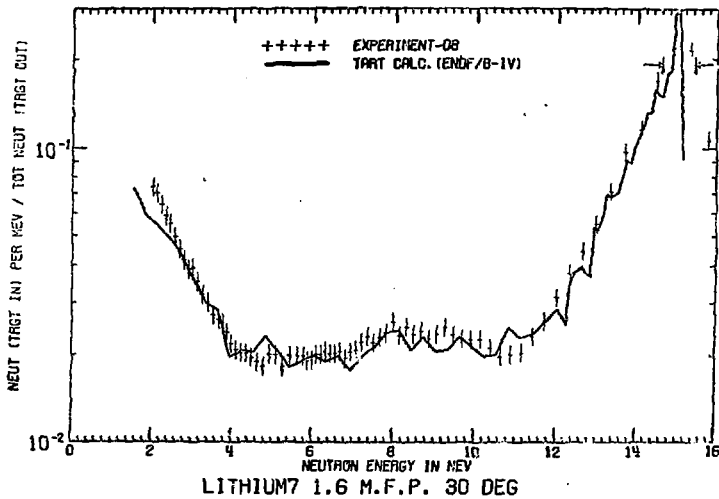
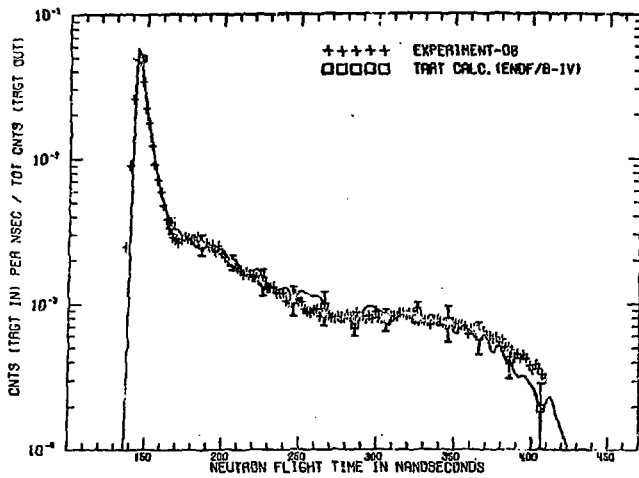


Fig. 6